

Conf - 910503 - 6

EVALUATION OF THE SILICON ISOTOPES FOR ENDF/B-VI

CONF-910503--6

D. M. Hetrick, D. C. Larson, N. M. Larson, C. Y. Fu, and S. J. Epperson

DE91 012053

Oak Ridge National Laboratory
P. O. Box 2008
Oak Ridge, TN 37831-6356 USA

Abstract: Isotopic evaluations for $^{28,29,30}\text{Si}$ performed for ENDF/B-VI are briefly reviewed. The evaluations are based on analysis of experimental data and results of model calculations. Evaluated data are given for neutron induced reaction cross sections, angular and energy distributions, and gamma-ray production cross sections. All necessary data are given to allow KERMA (Kinetic Energy Released in Materials) and displacement cross sections to be calculated directly from information available in the evaluations. These quantities are fundamental to studies of neutron heating and radiation damage.

($^{28,29,30}\text{Si}$ for ENDF/B-VI, cross sections, neutron heating, radiation damage)

MASTER

Introduction

Silicon is important for radiation damage studies and neutron and gamma-ray transport calculations. For ENDF/B-VI, separate evaluations were done for the three stable isotopes of silicon. The evaluations are based on analysis of experimental data, supplemented by results of nuclear model calculations. This paper summarizes the evaluations and notes the measured data considered and the model codes used. Examples of evaluations are compared to data.

Computational Methods and Procedures

The primary code used for this evaluation work was TNG [1], an advanced multistep Hauser-Feshbach model. TNG includes precompound and compound contributions to cross sections in a self-consistent manner, provides correlated angular and energy distributions, calculates gamma-ray production, and conserves angular momentum in all steps.

Calculations for $^{28,29,30}\text{Si}$ at a number of incident energies from 0.01 to 20.0 MeV were performed. Parameters required as input to TNG for the silicon isotopes are discussed in detail in [2]. The results from TNG are found to agree reasonably well with available data.

The resonance parameters are given in File 2 ENDF format for the evaluations. For File 3, when sufficient cross-section data were available, they were evaluated and used; otherwise calculations are used. Energy spectra for all outgoing particles, including photons, are given in File 6. Angular distributions are given for the neutron emission spectra for ^{28}Si only and isotropy is assumed for the other isotopes and particles. Branching ratios for the discrete levels are given directly in File 12; i.e., the continuum and discrete gammas are given separately. For the first time, all necessary nuclear data are given in the evaluations to allow direct computation of KERMA and displacement cross sections. These quantities are fundamental in studies of neutron heating and radiation damage.

Resonance Parameters

In the resonance region (thermal to 4 MeV), the available total [3,4,5] and inelastic [6,7] data for natural silicon, and total cross section data for $^{29,30}\text{Si}$ dioxide [6,7], were analyzed using the multilevel R-matrix code SAMMY [8]. Included in the analysis were thermal values of total [9], elastic [9], and capture [10] cross sections for all three silicon isotopes, and for oxygen. Resonance parameters used in ENDF/B-VI were derived from and are consistent with all these data.

Cross Sections

The total cross section in the resonance region is represented by resonance parameters for each isotope, taken from a SAMMY analysis of measured data. Above the resonance region there are no new isotopic data, so extensive checks were done comparing the ENDF/B-V total cross section with recent data for ^{28}Si . Based on these comparisons, the ENDF/B-V results were retained. Details are given in [2].

The nonelastic cross section is the sum of all reaction processes except elastic scattering; the elastic cross section is derived by subtracting the nonelastic from the total.

Inelastic scattering data to the 1.779- and 4.617-MeV levels were taken from ENDF/B-V and were based on measurements [2]. Inelastic scattering data to higher states in ^{28}Si are sparse, and evaluated cross sections for these levels (up to 8 MeV) are from the TNG calculation. A direct interaction component was included for the 6.276-, 6.879-, and 6.889-MeV levels.

Discrete inelastic levels up to 6.0 MeV in ^{29}Si and 5.0 MeV in ^{30}Si were included in the respective evaluations. The TNG analyses were used exclusively since there are no available cross-section data.

The (n, p) cross section for ^{28}Si is based on measurements from threshold to 9 MeV; TNG results are used from 9 to 20 MeV. Cross sections are given for individual levels up to 3 MeV in the residual nucleus ^{28}Al , again based on calculation and using available data as a guide. Results for $^{28}\text{Si}(n, p)^{28}\text{Al}$ are shown in Fig. 1; the TNG calculations (for $E_n > 9.0$ MeV) are a good compromise.

From threshold to 8.4 MeV, the evaluation of Drake [11] is adopted for the $^{28}\text{Si}(n, \alpha)^{25}\text{Mg}$ reaction. Above 8.4 MeV, TNG is used as other alpha particle groups are contributing to the cross section but can not be resolved. Cross sections are given for levels up to 4.8 MeV in the residual nucleus ^{25}Mg , based on TNG and using data as a guide. TNG calculations are used for $^{29}\text{Si}(n, p)$, $^{29}\text{Si}(n, \alpha)$, $^{30}\text{Si}(n, p)$ and $^{30}\text{Si}(n, \alpha)$ as the measurements are quite discrepant and TNG offers a good compromise.

There have been no new measurements of the (n, d) reaction since the evaluation of Drake [11], so that work is adopted. Few data exist for tertiary reaction cross sections of the silicon isotopes and thus TNG results are used.

Angular Distributions

Angular distributions of secondary neutrons for elastic scattering are taken from ENDF/B-V [2]. For the discrete levels at 1.779, 4.617, 6.276, 6.879, and 6.889 MeV in ^{28}Si , the angular distributions in ENDF/B-VI are a weighted sum of the Legendre coefficients from the TNG

DISCLAIMER

This report was prepared as an account of work sponsored by an agency of the United States Government. Neither the United States Government nor any agency thereof, nor any of their employees, makes any warranty, express or implied, or assumes any legal liability or responsibility for the accuracy, completeness, or usefulness of any information, apparatus, product, or process disclosed, or represents that its use would not infringe privately owned rights. Reference herein to any specific commercial product, process, or service by trade name, trademark, manufacturer, or otherwise does not necessarily constitute or imply its endorsement, recommendation, or favoring by the United States Government or any agency thereof. The views and opinions of authors expressed herein do not necessarily state or reflect those of the United States Government or any agency thereof.

and DWUCK calculations. The angular distributions for all other levels of $^{28,29,30}\text{Si}$ were taken from TNG results.

Energy-Angle Correlated Distributions

The computed angular distributions of neutron production cross sections for silicon at $E_n = 14.5$ MeV and for three outgoing energy bins are compared with experiments in Fig. 2. The results for $E'_n = 7.0 - 8.0$ MeV are in the discrete region and include the sum of TNG and DWUCK calculations. For $E'_n = 6.0 - 7.0$ MeV, the results are also in the discrete region but are symmetric since there was no direct interaction contribution.

Neutron emission measurements are available only for incident energies from 14.0 to 14.6 MeV and there are no charged particle production measurements. Particle emission spectra were computed via TNG for 35 incident energies for each silicon isotope. The computed neutron spectra at $E_n = 14.5$ MeV (weighted sum of $^{28,29,30}\text{Si}$) are compared with the natural silicon measured data in Fig. 3.

It appears that the calculated neutron emission is too small at low outgoing energies. Experimentally, low energy neutrons form the largest part of the background, so background subtraction is quite difficult in this region of the spectrum. It has been observed that the data of Clayeux and Voignier [12] and Takahashi et al. [13] for several elements differ significantly at low energy from the data of Hermsdorf et al. [14] and others [15,16]. There is good overall agreement between experiment and calculation in the nonelastic cross section, the various partial reaction cross sections, and gamma-ray production spectra (see below). Since energy conservation must be satisfied, the computed neutron emission as shown in Fig. 3 is judged to be acceptable.

Prior to incorporation in File 6, the neutron and charged particle energy distributions from TNG were input to the RECOIL code [17], which converts the distributions from the center of mass to the laboratory frame, and computes the energy spectra of the heavy recoil nucleus. The recoil nucleus distributions are also entered in File 6; isotropy is assumed.

The calculated gamma-ray emission spectrum at 14.5 MeV is compared to measured data [18] in Fig. 4. The calculation provides a good reproduction of the data, and in addition provides information on the cross sections for $E_\gamma < 0.7$ MeV. The computed energy-dependent yield and the TNG normalized distributions for the gamma rays at several incident energies are given for each reaction using File 6 in ENDF/B-VI.

Uncertainty Information

Uncertainty files are given for all cross sections in File 3, but not for the resonance parameters, energy distributions, or angular distributions. Fractional and absolute components, correlated only within a given energy interval, are based on data and estimates of uncertainties associated with the model calculations (see Hetrick et al. [19]).

KERMA and Damage Calculations

Improvements to ENDF/B-VI for KERMA and damage calculations are discussed in Ref. [20]. Briefly, prior to ENDF/B-VI, evaluations did not contain spectral distributions for outgoing charged particles, so only approximations could be made for heating and KERMA. Now, the nuclear data are given to compute these quantities directly.

Summary and Conclusions

Advanced nuclear model codes, an improved experimental data base, more flexible ENDF formats, and isotopic evaluations were used for the evaluation of silicon

in ENDF/B-VI. Cross sections for all important reactions are included. Measurements are used to benchmark the calculations. Charged particle spectra are provided. Energy conservation is achieved to less than 1% for all reactions at all energies. The required data are given to allow KERMA and heating to be calculated directly from the evaluation.

This evaluation is much improved over ENDF/B-V. However, the evaluations would benefit from improving the data base further. For example, isotopic total cross section data need to be made available, particularly in the resonance region. Proton and alpha emission spectra are nonexistent and are needed to verify the model calculations, as well as neutron emission spectra at energies other than 14.5 MeV. Little or no data exist for the tertiary reactions with which to benchmark model calculations. Uncertainties should be given for important resonance parameters, and angular and energy distributions.

Acknowledgements

This research was sponsored by the office of Energy Research, Division of Nuclear Physics, U.S. Department of Energy, under contract DE-AC05-84OR21400 with Martin Marietta Energy Systems, Inc., and the Defense Nuclear Agency under Interagency Agreement Number 0046-C084-A1. Also, sincere thanks goes to Sue Damewood for typing this report and to Larry Weston and Bob Roussin for their helpful comments upon reviewing this paper.

References

1. C. Y. Fu, *Nucl. Sci. Eng.* **100**, 61 (1990).
2. D. C. Larson, D. M. Hetrick, N. M. Larson, C. Y. Fu, and S. J. Epperson, *Evaluation of $^{28,29,30}\text{Si}$ for ENDF/B-VI*, ORNL/TM-11825 (1991).
3. R. B. Schwartz, R. A. Schrack, and H. T. Heaton, *Bull. Amer. Phys. Soc.* **16**, 495 (1971).
4. H. Weigmann, P. W. Martin, R. Kehler, I. van Parijs, F. Poortmans, and J. A. Wartena, *Phys. Rev.* **C36**, 585 (1987).
5. D. C. Larson, C. H. Johnson, J. A. Harvey, N. W. Hill, *Measurement of the Neutron Total Cross of Silicon from 5 eV to 730 keV*, ORNL/TM-5618 (1976).
6. J. A. Harvey, private communication, ORNL, (1991)
7. J. A. Harvey, W. M. Good, R. F. Carlton, B. Castel, J. B. McGroarty, and S. F. Mughabghab, *Phys. Rev.* **C28**, 24 (1983).
8. N. M. Larson, *Updated Users' Guide for SAMMY: Multilevel R-Matrix Fits to Neutron Data Using Bayes' Equations*, ORNL/TM-9179/R2 (1989).
9. S. F. Mughabghab, *Neutron Cross Sections*, Academic Press, Inc. (1984).
10. M. A. Islam, T. J. Kennett, and W. V. Prestwich, *Phys. Rev.* **C41**, 1272 (1990).
11. M. K. Drake, Gulf General Atomic Report GA-S628 (1968).
12. G. Clayeux and J. Voignier, CEA Report CEA-R-4279 (1972).
13. A. Takahashi, J. Yamamoto, T. Murakami, K. Oshima, H. Oda, K. Fujimoto, M. Ueda, M. Fukazawa, Y. Yanagi, J. Miyaguchi, and K. Sumita, Octavian Rpt. A-83-01, Osaka Univ., Japan (1983).
14. D. Hermsdorf, A. Meister, S. Sassonoff, D. Seeliger, K. Seidel, and F. Shalgin, Zentralinstitut für Kernforschung Rossendorf Bei Dresden, ZfK-277 (U) (1975).
15. D. M. Hetrick, D. C. Larson, and C. Y. Fu, *Status of ENDF/B-V Neutron Emission Spectra Induced by 14-MeV Neutrons*, ORNL/TM-6637, ENDF-280 (1979).
16. C. Y. Fu and D. M. Hetrick, *Trans. Am. Nucl. Society* **53**, 409 (1986).

17. C. Y. Fu and D. M. Hetrick, Computer Code RE-COIL, ORNL, Unpublished (1985).
18. J. K. Dickens, T. A. Love, and G. L. Morgan, *Gamma-Ray Production from Neutron Interactions with Silicon for Incident Neutron Energies Between 1.0 and 20 MeV: Tabulated Differential Cross Sections*, ORNL-TM-4389 (1973).
19. D. M. Hetrick, D. C. Larson, and C. Y. Fu, Generation of Covariance Files for Isotopes of Cr, Fe, Ni, Cu, and Pb in ENDF/B-VI, ORNL/TM-11763 (1991).
20. D. C. Larson, D. M. Hetrick, C. Y. Fu, and S. J. Epperson, in *Proc. Seventh ASTM-EURATOM Symposium on Reactor Dosimetry, August 1990, Strasbourg, France* (Edited by G. Tsotridis), (1991).

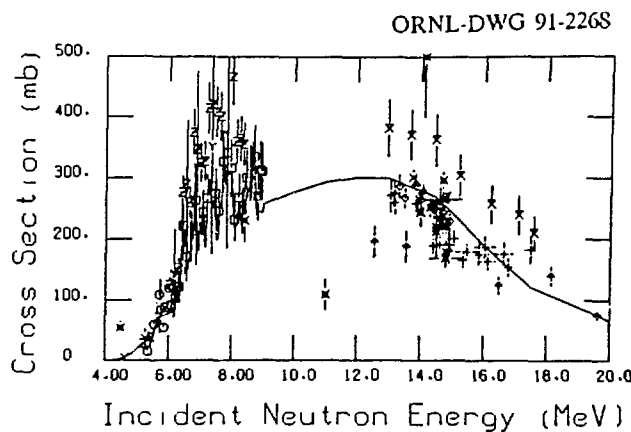


Fig. 1. $^{28}\text{Si}(n, p)$ in ENDF/B-VI compared to data (see Ref. 2.)

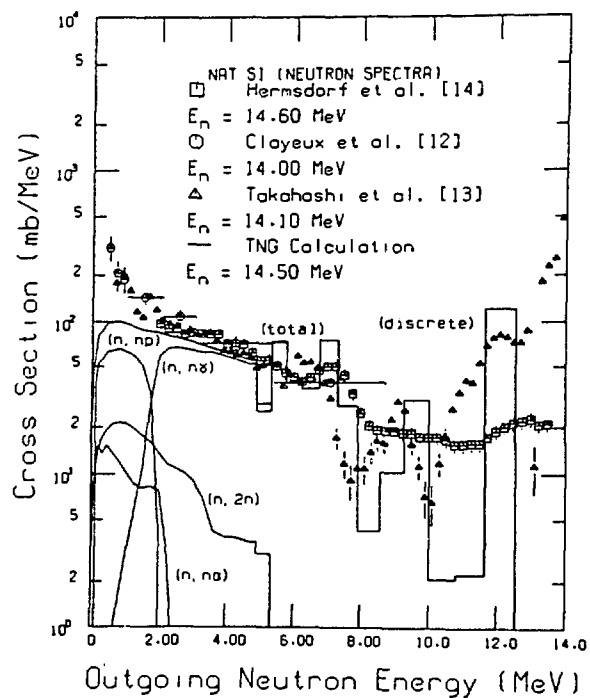


Fig. 3. Calculated neutron emission spectra compared to data.

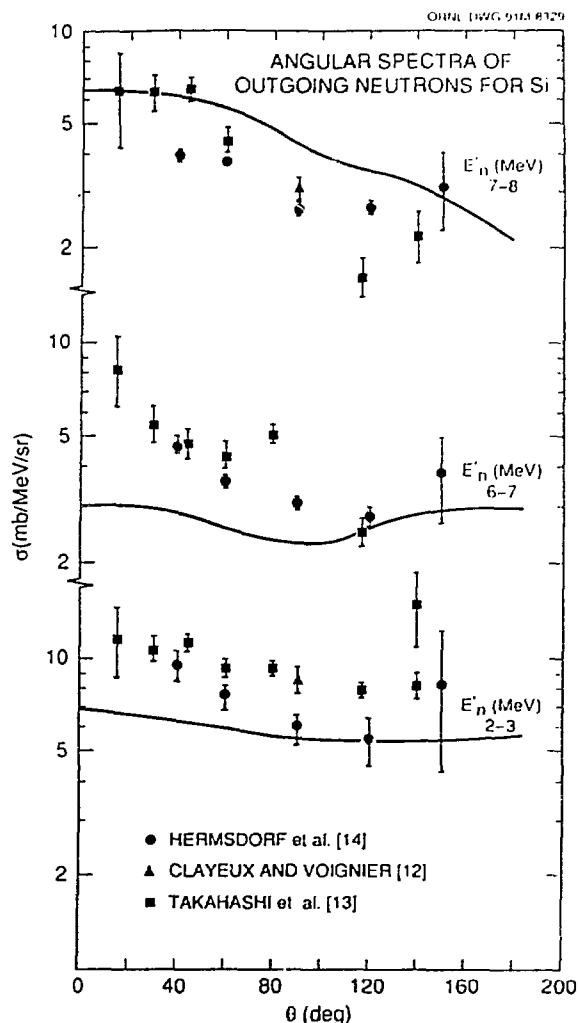


Fig. 2. Comparison of computed and measured neutron production cross sections.

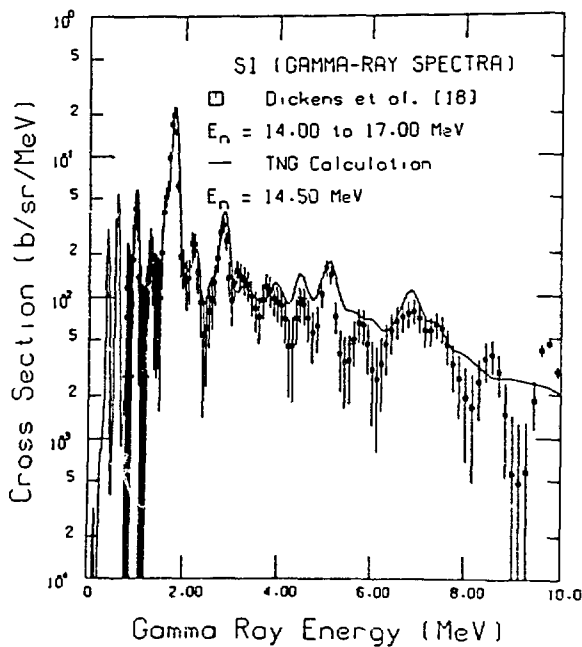


Fig. 4. Calculated gamma-ray spectra compared to data.